

The states of hydrogen and hydrogen embrittlement susceptibility of precipitation hardened SUS630 stainless steel

Y Hayashi^{1, a)}, T Ito² and Y Nishimura², K Takai^{3, b)}

¹Graduate Student, Sophia University, 7-1 Kioi-cho, Chiyoda-ku, Tokyo 102-8554

²Materials Engineering R&D Division, DENSO CORP.

³Department of Engineering and Applied Sciences, Faculty of Science and Technology, Sophia University

a) dog.tennis.y1109uc@gmail.com

b) takai-k@sophia.ac.jp

Abstract. To elucidate the influence of precipitates on the states of hydrogen and hydrogen embrittlement susceptibility of SUS630, solution treatment, sub-aging (410 °C, 1 h), peak-aging (470 °C, 1 h), and over-aging (550 °C, 1 h) methods were used to prepare specimens. States of hydrogen were analyzed by thermal desorption analysis (TDA). Hydrogen embrittlement susceptibility was evaluated using tensile tests. Specimens were electrochemically precharged with hydrogen and then tensile tests were carried out simultaneously with hydrogen charging under the same conditions as those after precharging. Susceptibility was evaluated as the elongation ratio with/without hydrogen. The solution-treated and sub-aged specimens displayed a single peak near 100 °C, whereas peak- and over-aged specimens displayed two peaks, one near 100 °C and the other near 200 °C. The peak near 100 °C corresponded to hydrogen desorbed from the matrix and the peak near 200 °C corresponded to hydrogen desorbed from Cu precipitates. Ductility of peak- and over-aged specimens with hydrogen did not decrease, however, that of solution-treated and sub-aged specimens with hydrogen did. These findings indicate that specimens containing hydrogen with a higher temperature peak associated with Cu precipitates showed less hydrogen embrittlement susceptibility than those containing hydrogen with only a lower temperature peak.

1 Introduction

It has been reported that nanosize precipitates were observed in steel specimens by adding Cu and performing aging treatment [1, 2]. In recent years, precipitation strengthening by Cu precipitates has attracted attention in that it can improve the balance between strength and ductility of steel materials. Though hydrogen embrittlement can occur in high strength materials, Cu precipitates may improve resistance to it by trapping hydrogen in the same way as Ti and V carbides [3-5]. However, the hydrogen trapping capacity and hydrogen embrittlement susceptibility of Cu precipitates have been poorly understood to date. In addition, it is also expected that the hydrogen trapping capacity changes by increasing the aging temperature because the coherence of the precipitate-matrix interface changes with the crystal structure of the transforming precipitates. In this study, we investigated the influence of precipitates on the states of hydrogen and hydrogen embrittlement susceptibility of SUS630 under various aging conditions.



2 Experimental.

2.1 Material

The chemical composition of the specimens is listed in Table 1. Four kinds of specimens with different aging treatments were prepared (solution-treated, sub-, peak-, and over-aged specimens). The aging conditions and the tensile strengths are shown in Table 2. Two kinds of test pieces were prepared with different shapes. Cylindrical test pieces (10 mm diameter, 0.8 mm thick) were prepared for the analysis of the states of hydrogen. Specimens were prepared as shown in Fig. 1 for use in evaluating hydrogen embrittlement susceptibility.

2.2 Analysis of States of Hydrogen

The specimen surface was mechanically polished using emery paper (#800, 1000 and 2000). TDA was applied to the cylindrical specimens (0.8 mm thickness and 10 mm diameter). Hydrogen charging into the specimens was carried out by immersion in a 10 mass % NH_4SCN solution maintained at 30 °C for 48 h until hydrogen reached equilibrium at the center of the specimens. Immediately after hydrogen charging, the hydrogen content was analyzed by thermal desorption analysis (TDA) using a gas chromatograph calibrated with a standard gas containing 50 vol ppm of hydrogen in Ar used as a detection system. The temperature was raised from room temperature to 400 °C at 100 °C · h⁻¹.

2.3 Evaluation of Hydrogen Embrittlement Susceptibility

Hydrogen embrittlement susceptibility was evaluated in tensile testing. Two methods, tensile testing and TDA, were applied to the specimens as shown in Fig.1. They were electrochemically precharged with hydrogen in a 0.1N NaOH solution maintained at various current potentials (-0.9 - -2.0 V vs Ag/AgCl) and then tensile tests were carried out at a crosshead speed of 0.09 mm · min⁻¹ and a temperature of 30 °C with/without hydrogen precharging. To keep the hydrogen concentration inside the specimen constant during tensile testing, the tests were conducted simultaneously with hydrogen charging under the same conditions as those after hydrogen precharging. Susceptibility was evaluated as the elongation ratio with/without hydrogen. The hydrogen content was analyzed by TDA. In this study, tensile tests were carried out under two conditions, which were a low hydrogen content (hydrogen charged at -0.9 - -1.0 V vs Ag/AgCl) and a high hydrogen content (hydrogen charged at -1.2 - -1.5 V vs Ag/AgCl), so as to evaluate the influence between the states of hydrogen and hydrogen embrittlement susceptibility. The fracture surfaces were observed using a field emission scanning electron microscope (FE-SEM).

Table 1. Chemical composition of SUS630 specimen (mass %).

C	Si	Mn	P	S	Cu	Ni	Cr	Nb+Ta
0.05	0.24	0.86	0.034	0.004	3.32	4.25	15.66	0.24

Table 2. Heat treatment conditions and tensile strength of SUS630 specimens (MPa).

	Solution	Sub-aged	Peak-aged	Over-aged
ST	1050 °C	1050 °C	1050 °C	1050 °C
AT	—	410 °C	470 °C	550 °C
TS	1160 MPa	1265 MPa	1421 MPa	1168 MPa

3 Results and Discussion.

3.1 States of hydrogen in SUS630

Figure 2 shows the TDA profiles of hydrogen added by immersion in a 10 mass % NH_4SCN solution maintained at 30 °C for 48 h. The results show that the solution-treated and sub-aged specimens had a single peak near 100 °C, whereas the peak- and over-aged specimens had two peaks, one near 100 °C and the other one near 200 °C. It has been reported that hydrogen desorbed near 100 °C is trapped at atomic vacancies, the elastic stress field around the dislocation core, the dislocation core, and grain boundaries in the matrix of medium-carbon tempered martensitic steel [6, 7]. In the case of the tested martensitic stainless steel SUS630, the peak near 100 °C presumably corresponded to hydrogen desorbed from the same trapping sites. The peak near 200 °C corresponded to hydrogen desorbed from Cu precipitates because it appeared with increasing aging temperature. In addition, the peak near 200 °C did not appear in the case of sub-aged specimens. These findings indicate that the states of Cu precipitates affected the hydrogen trapping capacity.

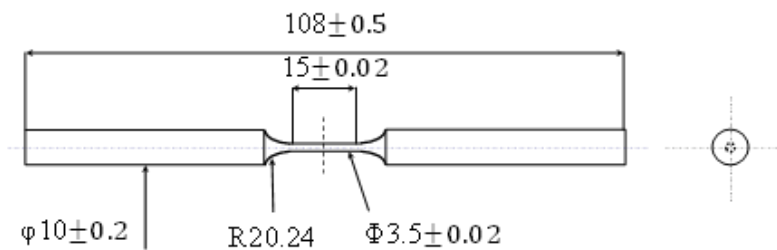


Fig. 1 Geometry and dimensions of specimen for the tensile tests.

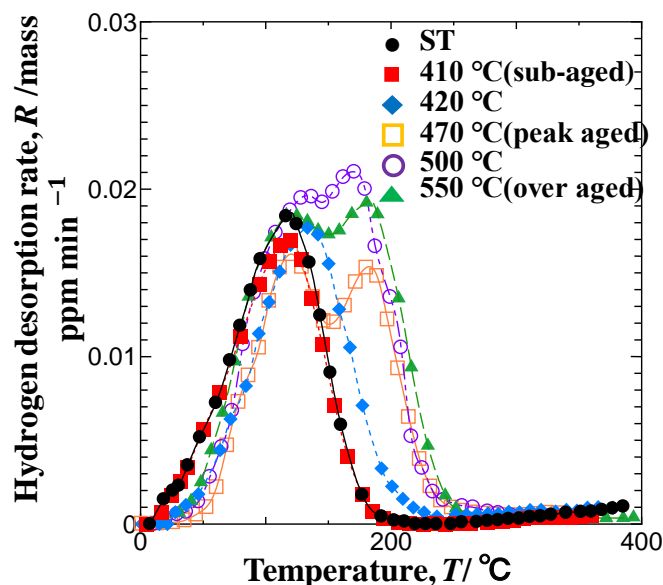


Fig. 2 Hydrogen desorption profiles of specimens immersed for 48 h in a 10 mass% NH_4SCN solution at a temperature of 30 °C for various aging temperatures.

3.2 Hydrogen Embrittlement Susceptibility in SUS630

3.2.1 Change in Ductility with/without Hydrogen

Figure 3 and Figure 4 show nominal stress-strain curves at a crosshead speed of $0.09 \text{ mm} \cdot \text{min}^{-1}$ under low and high hydrogen content conditions, respectively, for (a) solution-treated, (b) sub-aged, (c) peak-aged, and (d) over-aged specimens. The tensile test results show that the ductility of peak- and over-aged specimens did not decrease, whereas the ductility of solution-treated and sub-aged specimens decreased under a low hydrogen content. At a high hydrogen content, the ductility of all specimens clearly decreased.

3.2.2 TDA profiles of Tensile Testing

TDA profiles under low and high hydrogen content conditions are shown in Fig. 5 and Fig. 6, respectively. The results indicate that hydrogen was trapped in the matrix of solution-treated and sub-aged specimens under a low hydrogen content, whereas it was mainly trapped in the Cu precipitates of peak- and over-aged specimens. Peak separations were attempted using the Gaussian function to ascertain the states of hydrogen under a high hydrogen content for further investigation. As a result, peaks were separated into two peaks consisting of one at $137 \text{ }^\circ\text{C}$ and the other one at $233 \text{ }^\circ\text{C}$. Hydrogen was trapped not only in the Cu precipitates but also in the matrix of peak- and over-aged specimens. For these reasons, when hydrogen is trapped only in the precipitates, there is probably an effect of suppressing hydrogen embrittlement. However, that effect disappears when hydrogen is trapped not only in the precipitates but also in the matrix.

3.2.3 Fracture Surface Observation

Figure 7 and Figure 8 show photographs of fracture surfaces observed by the FE-SEM under the low and high hydrogen content conditions, respectively. Under a low hydrogen content, a quasi-cleavage fracture surface was observed in (a) solution-treated and (b) sub-aged specimens that showed hydrogen embrittlement, whereas (c) peak-aged and (d) over-aged specimens displayed a fracture surface with microvoid coalescence. Under a high hydrogen content, a quasi-cleavage fracture surface was observed for all aged specimens. An intergranular fractured surface was observed for over-aged specimens.

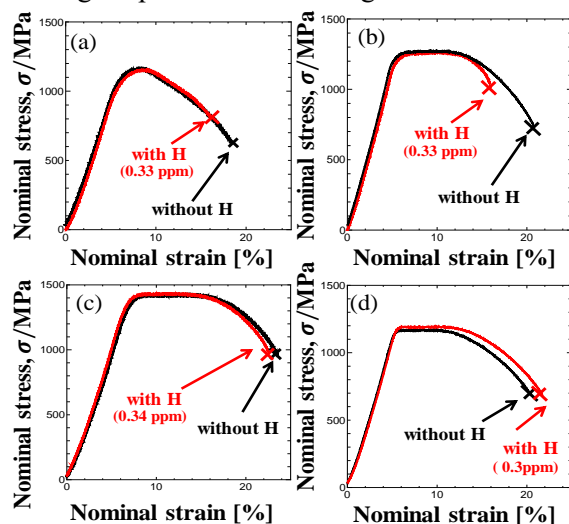


Fig. 3 Nominal stress-strain curves with/without hydrogen charging at -0.9 - -1.0 V vs Ag/AgCl in a 0.1N NaOH solution at a temperature of $30 \text{ }^\circ\text{C}$. (a) Solution-treated, (b) sub-aged, (c) peak-aged and (d) over-aged specimens.

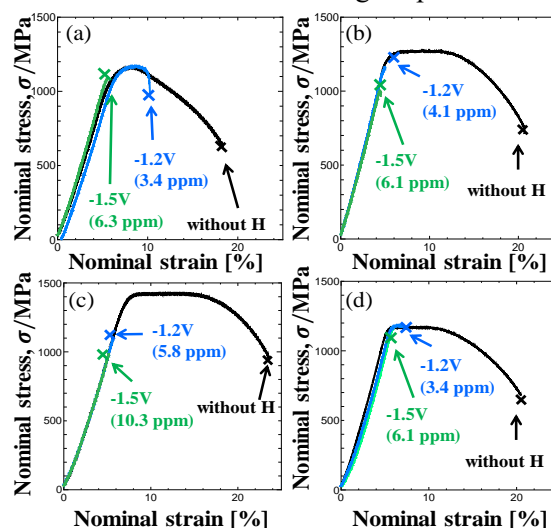


Fig. 4 Nominal stress-strain curves with/without hydrogen charging at -1.2 - -1.5 V vs Ag/AgCl in a 0.1N NaOH solution at a temperature of $30 \text{ }^\circ\text{C}$. (a) Solution-treated, (b) sub-aged, (c) peak-aged and (d) over-aged specimens.

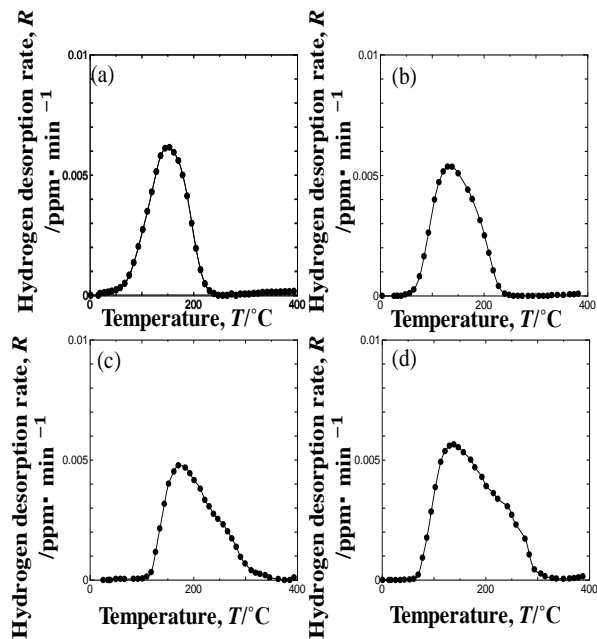


Fig. 5 Hydrogen desorption profiles of hydrogen-charged at -0.9 - -1.0 V vs Ag/AgCl in 0.1N NaOH solution at a temperature of 30 °C. (a) Solution-treated, (b) sub-aged, (c) peak-aged and (d) over-aged specimens.

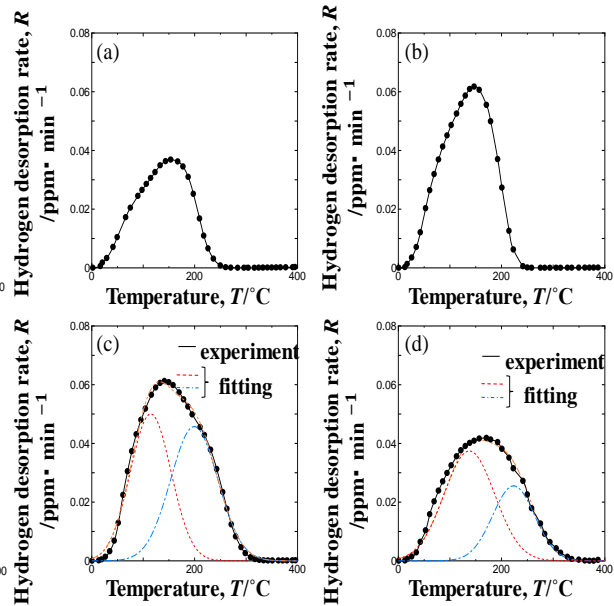


Fig. 6 Comparison of thermal desorption profiles between experiment and fitting using the Gaussian function of hydrogen - charged at -1.2 V vs Ag/AgCl in 0.1N NaOH solution at a temperature of 30 °C. (a) Solution-treated, (b) sub-aged, (c) peak-aged and (d) over-aged specimens.

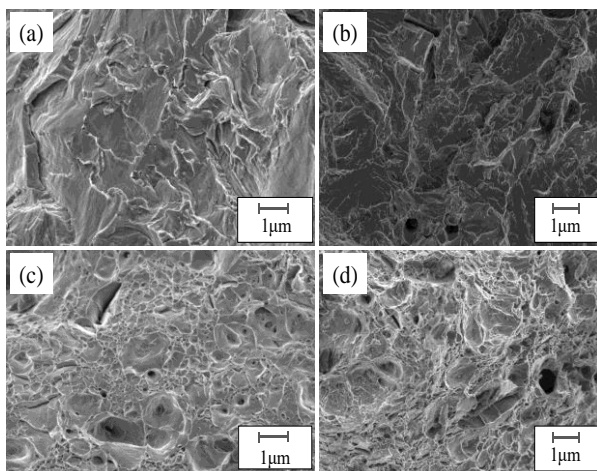


Fig. 7 Microscopic fracture surfaces with/without hydrogen charging at -0.9 - -1.0 V vs Ag/AgCl in a 0.1N NaOH solution at a temperature of 30°C. (a) Solution-treated, (b) sub-aged, (c) peak-aged and (d) over-aged specimens.

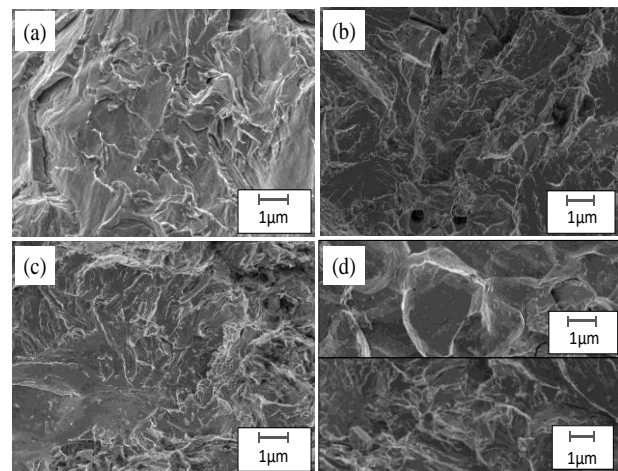


Fig. 8 Microscopic fracture surfaces with/without hydrogen charging at -1.2 V vs Ag/AgCl in a 0.1N NaOH solution at a temperature of 30 °C. (a) Solution-treated, (b) sub-aged, (c) peak-aged and (d) over-aged specimens.

4 Conclusion

- (1) Solution-treated and sub-aged specimens displayed a single peak near 100 °C, whereas peak- and over-aged specimens displayed two peaks, one near 100 °C and the other one near 200 °C. The peak near 100 °C corresponded to hydrogen desorbed from the matrix and the peak near 200 °C corresponded to hydrogen desorbed from Cu precipitates.
- (2) Ductility of peak-aged and over-aged specimens was not decreased, however, ductility of solution-treated and sub-aged specimens was decreased under low hydrogen content. With high hydrogen content, ductility of all specimens were decreased.
- (3) When hydrogen was trapped only in precipitates, there was the effect of suppressing hydrogen embrittlement. However, that effect was disappeared when hydrogen was trapped both in precipitates and matrix.

5 References

- [1] Goodman R S, Brenner S S and Low J R Jr 1973 *Metallurgical and Materials Transactions* **4** 2363.
- [2] Osamura K, Okuda H, Takashima M, Asano K and Furusaka M 1993 *Materials Transactions* **34** 305.
- [3] Hirth P J 1980 *Materials Transactions A* **11A** 861.
- [4] Tsuchida T, Hara T and Tsuzaki K 2002 *Tetsu to Hagane* **88** 771.
- [5] Yokota T and Shiraga T 2003 *The Iron and Steel Institute of Japan* **43** 534.
- [6] Takai K 2011 *Zairyo-to-Kankyo* **60** 230.
- [7] Koyama M, Rohwerder M, Tasan Cem C, Bashir A, Akiyama E, Takai K, Raabe D & Tsuzaki K 2017 *Material Science and Technology* **33** 1483.